Open Journal of Applied Sciences, **2013, 3, 490-513**
Published Online December 2013 (http://www.scirp.org/journal/ojapps)
http://dx.doi.org/10.4236/ojapps.2013.38059

Numerical Analysis of the Analytical Relationships between Angstrom Coefficients of Aerosols and Their Optical Properties for Four Types of Aerosols

Bello Idrith Tijjani[1], Sha'aibu Uba[2], Fatima Salman Koki[1]
[1]Department of Physics, Bayero University, Kano, Nigeria
[2]Department of Physics, Ahmadu Bello University, Zaria, Nigeria
Email: idrith@yahoo.com, idrithtijjani@gmail.com, shuba356@yahoo.com, shuba356@yahoo.com, FatimaSK2775@gmail.com

Received September 30, 2013; revised November 2, 2013; accepted November 10, 2013

ABSTRACT

In this paper, the authors numerically analyzed the analytical relationships between angstrom coefficients and optical properties of aerosols to the existing data extracted from OPAC at the spectral length of 0.25 μm to 2.5 μm at eight relative humidity for desert, urban, marine clean and continental clean aerosols. That is apart from their relationships with the wavelength that was determined, in this paper their relation with respect to aerosols' type and RHs are determined. The properties extracted are scattering, absorption, and extinction coefficients and single scattering albedo. The results showed that the extinction and single scattering albedo are correct for all the aerosols but single scattering co-albedo is satisfied for only sahara and continental clean.

Keywords: Angstrom Coefficients; Analytical Relationships; Parameterize; Wavelength Dependence; Optical Properties

1. Introduction

The Angstrom exponent (AC) is a parameter that is being widely used in atmospheric sciences to analyze the optical properties of aerosol particles. Since the early publications of Angstrom [1,2] and his later publications [3,4], where this parameter was mainly applied to the description of the spectral behavior of the atmospheric extinction and transmission, respectively, it is now being applied to a variety of similar but slightly different optical properties, for instance to the atmospheric, optical depth, extinction coefficient, scattering or backscattering coefficients etc. It is very popular not only because of the simplicity of the equation, but because it enables extrapolation or interpolation of aerosols' optical properties, because it is connected to particle microphysics (related with the mean size of aerosols) as it describes, approximately for a certain radius range, and a spectral range, a power law (Junge) aerosol size distribution [5-8]. It was refined by O'Neill and Royer [9] who derived bimodal size distribution radii using these parameters.

The Angstrom exponent being an indicator of the aerosol spectral behaviour of aerosols [10], has been adopted by a number of authors in the literature to characterize biomass burning aerosols [11,12], urban and desert dust aerosol [13] and maritime aerosols [14]. In general, the aerosol optical depth (AOD) and AC parameters can be used to differentiate between coarse and fine particles [15].

Simple analytical relationships between extinction, scattering, and absorption coefficients and single scattering albedo (*SSA*) [16], and the corresponding relationships for *AC*s [17] exist. Such relationships are useful to compare *AC*s obtained from extinction, scattering, and absorption, including the ground truthing of remote sensing and satellite measurements. For example, aerosol extinction can be obtained from ground-based and satellite remote sensing at multiple wavelengths yielding extinction Angstrom coefficients (*EAC*s). Simple analytical relationships between *EAC*s, scattering Angstrom coefficients (*SAC*s), and absorption Angstrom coefficients (*AAC*s)

will help attribute the *EAC*s to the underlying physical phenomena, namely scattering and absorption, and analyzing closure between the different Angstrom coefficients. In addition, *SSA* is the key parameter that normally determines the sign and magnitude of aerosol radiativeforcing. *SSA* can be obtained at multiple wavelengths from in-situ measurements [7,8,18], ground-based remote sensing measurements [19,20], and potentially from satellite measurements [21,22]. Relating the *SSA* Angstrom coefficient (*SSAAC*) to the underlying *SAC*, *AAC*, and *EAC* will help with data interpretation and closure and physical understanding. The *SSA*s are some of the most dominant input factors that determine the aerosols type in radiative transfer models [23-26] and depend on the microphysical properties of the aerosols and therefore their value can be used for the characterization of the aerosol type. *SSA* can be interpreted as the probability that light will be scattered, giving an extinction event or the ratio between the scattering coefficient and the extinction coefficient while the Single scattering co-albedo (*SSCA*) can be considered as the probability of absorption per extinction event or ratio between the absorption coefficient and the extinction coefficient. Therefore if *SSAAC* is less than 0 it indicates that *SSA* increases with wavelength, while if *SSAAC* is larger than 0, *SSA* decreases with wavelength. This shows that *SSAAC* can be used to determine the increase or decrease in the radiative forcing and while for single scattering co-albedo Angstrom coefficient (*SSCAAC*) is the reverse. From the various plots we observed some spectral intervals where *SSA* decreases with the wavelength as well as some spectral intervals where *SSA* increases with the wavelength.

In addition, *AC*s can be obtained from simple linear or nonlinear regression of data plotted on a log-log scale or more complicated non-linear fits of data that may also yield higher order terms which give additional information about the type of aerosols using the curvature [27]. Relationships between different *AC*s that include the *SSA* (ω) have only been derived by Moosmuller and Chakrabarty, [17]as for single- and two-wavelength *AC*s, while for *AC*s obtained from linear or non-linear fits the mathematics gets much more complicated due to the difficulty of appropriately attributing the influence of the *SSA* at different wavelengths. However, in most cases, the single-wavelength equations still give a good approximation depending on the type of aerosols and relative humidity.

In aerosol optics, the *AC*s that are of most interest are scattering, absorption, and extinction coefficients and for the *SSA* (ω) and single scattering co-albedo (*SSCA*). The relationships between these *AC*s are analytically determined by Moosmuller and Chakrabarty, [17] as:

Extinction Angstrom coefficient *EAC*

$$EAC(\lambda) = AAC(\lambda) + \omega(\lambda)\left[SAC(\lambda) - AAC(\lambda)\right] \quad (1)$$

Single Scattering Albedo (*SSA*) Angstrom coefficient (*SSAAC*)

$$SSAAC(\lambda) = SAC(\lambda) - EAC(\lambda) \quad (2)$$

Single Scattering Co-Albedo (*SSCA*) Angstrom coefficient (*SSCAAC*)

$$SSCAAC(\lambda) = AAC(\lambda) - EAC(\lambda) \quad (3)$$

As suggested by Moosmuller and Chakrabarty [17], in this paper we are going to apply these relationships to the existing data extracted from OPAC at the spectral length of 0.25 μm to 2.5 μm and eight RHs (0%, 50%, 70%, 80%, 90%, 95%, 98%, and 99%) for desert, urban, marine clean and continental clean to determine its accuracy and its dependence on the types of aerosols, the power of the polynomials and RHs (that is hygroscopic growth as a result of the change in RHs).

2. Methodology

The models extracted from OPAC are given in **Table 1**.

The spectral behavior of the aerosol's optical parameter (X, say), with the wavelength of light (λ) is expressed as inverse power law [3]:

Table 1. Compositions of aerosol types [28].

Aerosol model types	Components	Concentration N_i (cm^{-3})
Urban	WASO	28000.0
	INSO	1.5
	SOOT	130000.0
	Total	158001.5
Continental clean	WASO	2600.0
	INSO	0.15
	Total	26000.15
Desert	WASO	2000.0
	MINM	269.5
	MIAM	30.5
	MICM	0.142
	Total	2300.142
Maritime clean	WASO	1500.0
	SSAM	20.0
	SSCM	0.0032
	Total	1520.0032

where: N_i is the mass concentration of the component, water soluble components (WASO, consists of scattering aerosols, that are hygroscopic in nature, such as sulfates and nitrates present in anthropogenic pollution), water insoluble (INSO), soot (SOOT, not soluble in water and therefore the particles are assumed not to grow with increasing relative humidity), mineral nucleation mode (MINM), mineral accumulation mode(MIAM) , mineral coarse mode (MICM), Sea salt accumulation mode (SSAM) and Sea salt coarse mode (SSCM). Urban aerosol represents strong pollution in urban areas. Continental clean aerosol represents remote continental areas without or with very low anthropogenic influences. Desert aerosol is used to describe aerosol over all deserts of the world, and no distinction with respect to the local properties is made. It consists of the mineral aerosol components in a combination that is representative for average turbidity, together with a certain part of the water-soluble component. Maritime aerosol types contain sea salt particles and Maritime clean is given to represent undisturbed remote maritime conditions with no soot, but with a certain amount of water-soluble aero-sol, which is used to represent the non-sea salt sulfate.

$$X(\lambda) = \beta\lambda^{-\alpha} \quad (4)$$

where X(λ) can represent extinction, scattering, and absorption coefficients, single scattering albedo and single scattering co-albedo while β is the turbidity and α is the Angstrom exponent (*AC*) [9,29]. The wavelength dependence of X(λ) can be characterized by the *AC*, which is a coefficient of the following regression:

$$\ln X(\lambda) = -\alpha \ln(\lambda) + \ln\beta \quad (5)$$

However the Angstrom exponent itself varies with wavelength, and a more precise empirical relationship between aerosol extinction and wavelength is obtained with a 2nd-order polynomial [13,30-38] as:

$$\ln X(\lambda) = \alpha_2 (\ln\lambda)^2 + \alpha_1 \ln\lambda + \ln\beta \quad (6)$$

Here, the coefficient α_2 accounts for a "curvature" often observed in sunphotometry measurements. Eck *et al*. [12,13], Schuster *et al*., [27], O' Neill *et al*., [34] and Kaskaoutis *et al*., [39,40] reported the existence of negative curvatures for fine-mode aerosols and near zero or positive curvatures are characteristic of size distributions with a dominant coarse-mode or bimodal distributions with coarse-mode aerosols having a significant relative magnitude.

Now differentiating Equation (5) with respect to lnλ we obtained

$$\alpha = -\frac{d(\ln X(\lambda))}{d(\ln(\lambda))} \quad (7)$$

Also differentiating Equation (6) with respect to lnλ we obtained

$$\frac{d(\ln X(\lambda))}{d(\ln(\lambda))} = \alpha_1 + 2\alpha_2 \ln(\lambda) \quad (8)$$

Assuming that Equations (7) and (8) are evaluated at a wavelength, this implies we can substitute Equation (7) into (8) to obtain

$$\alpha 1(\lambda) = -\alpha_1 - 2\alpha_2 \ln(\lambda) \quad (9)$$

Equation (9) now shows the relationship between α and wavelength.

We now also proposed a cubic relation of the form

$$\ln X(\lambda) = \ln\beta + \alpha_1 \ln\lambda + \alpha_2 (\ln\lambda)^2 + \alpha_3 (\ln\lambda)^3 \quad (10)$$

to determine whether cubic relation can improve the accuracy of Equations (1)-(3).

Also differentiating Equation (10) with respect to lnλ we obtained

$$\frac{d(\ln X(\lambda))}{d(\ln(\lambda))} = \alpha_1 + 2\alpha_2 \ln(\lambda) + 3\alpha_3 (\ln(\lambda))^2 \quad (11)$$

Assuming that Equations (7) and (11) are evaluated at a wavelength, this implies we can substitute Equation (7) into (11) to obtain

$$\alpha 2(\lambda) = -\alpha_1 - 2\alpha_2 \ln(\lambda) - 3\alpha_3 (\ln(\lambda))^2 \quad (12)$$

In this paper we are going to determine the correlation of Equations (1)-(3) with Equations (7), (9) and (12) for all the four types of the aerosols with respect to wavelengths and RHs. In Equation (1) since it involves products, we determined the average, but in Equations (2) and (3), since they have linear relations, we compared the coefficients.

3. Results and Observations

Figure 1(a) shows that power law is satisfied at 90%, 95%, 98% and 99% RH, but not satisfied at 0%, 50%, 70%, and 80%.

Table 2(a) shows good correlations at 90%, 95%, 98% and 99% RH, but bad correlations 0%, 50%, 70%, and 80% RH for linear. The increase in the power of the polynomials and RHs caused increase in the correlations.

Figure 1(b) shows that the plots can be approximated by the power law.

Table 2(b) shows very good correlations, and the correlations increase with the increase in the power of the polynomials and RHs.

Figure 1(c), spectral extinction coefficients decrease with wavelength and can be approximated with a power-law wavelength dependence and also a bi-modal type of particle size distributions [13]. The increase of the coefficients with RH has occurred because of the increase in mode size as a result of the increase in RHs. The increase of the extinction with RH at the deliquescence point (90 to 99) is that the growth increase substantially, making the process strongly nonlinear with RH [41,42].

Table 2(c) shows good correlations between extinction and λ using Equations (5), (6) and (10). The correlations increase with the increase in the power of the polynomials and RHs.

Observing **Figures 1(a)** and **Table 2(a)**, it can be seen that at RHs 0% to 90% the scattering coefficients have not satisfied the power law, and within this range it can be observed that in **Table 2(d)**, Equation (1) underestimated Equation (7) on the linear part but overestimated Equations (9) and (12) on the quadratic and cubic part respectively at all the RHs. The gaps decrease with the increase in RHs.

Figure 1(d) shows that the plots can be barely approximated by the power law.

Table 2(e) shows that the correlations decrease with the increase in RH, but increase with the increase in the power of the polynomials.

Comparing the coefficients at **Tables 2(e)** and **(f)** it

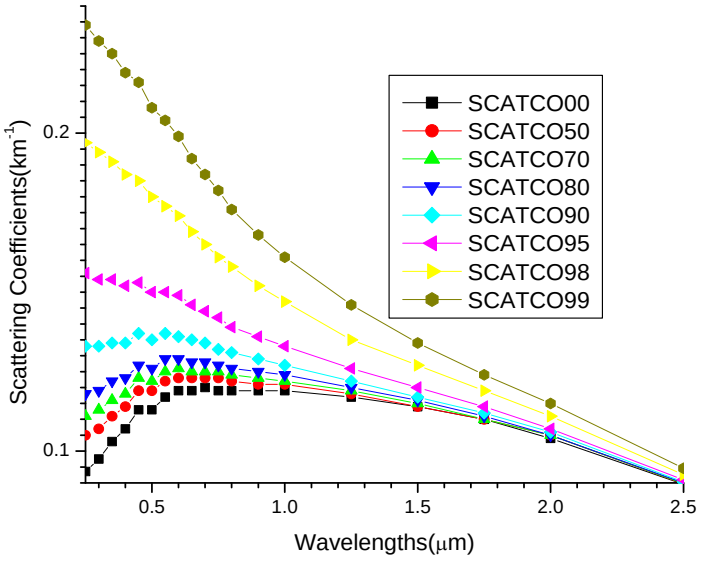

Figure 1(a). A graph of scattering coefficients against wavelength for sahara at RHs 0%, 50%, 70%, 80%, 90%, 95%, 98% and 99%.

Table 2(a). The results of the Angstrom coefficients of scattering coefficients using Equations (5), (6) and (10) for sahara model at the respective relative humidities using regression analysis with SPSS16.0.

RH	Linear Equation (5)		Quadratic Equation (6)			Cubic Equation (10)			
(%)	R^2	α	R^2	α_1	α_2	R^2	α_1	α_2	α_3
0	0.0053	−0.0101	0.9653	−0.0819	−0.2002	0.9829	−0.0515	−0.2349	−0.0455
50	0.0800	0.0355	0.9537	−0.1153	−0.1738	0.9805	−0.0812	−0.2127	−0.0510
70	0.2250	0.0606	0.9551	−0.1349	−0.1617	0.9817	−0.1002	−0.2012	−0.0518
80	0.3960	0.0853	0.9606	−0.1547	−0.1511	0.9839	−0.1203	−0.1903	−0.0515
90	0.6899	0.1389	0.9754	−0.1997	−0.1324	0.9890	−0.1673	−0.1694	−0.0485
95	0.8629	0.2082	0.9887	−0.2624	−0.1179	0.9937	−0.2362	−0.1478	−0.0392
98	0.9377	0.3124	0.9961	−0.3655	−0.1156	0.9967	−0.3522	−0.1307	−0.0198
99	0.9488	0.3841	0.9978	−0.4435	−0.1293	0.9978	−0.4399	−0.1335	−0.0055

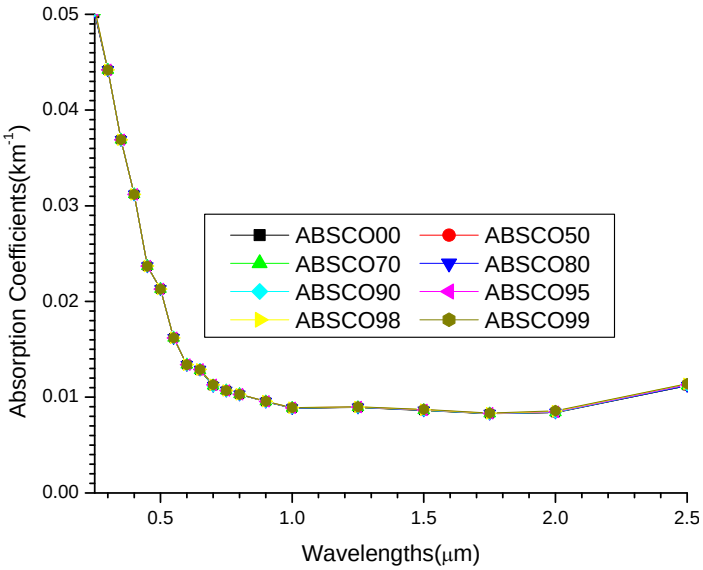

Figure 1(b). A graph of absorption coefficients against wavelength for sahara at RHs 0%, 50%, 70%, 80%, 90%, 95%, 98% and 99%.

Table 2(b). The results of the Angstrom coefficients of absorption coefficients using Equations (5), (6) and (10) for sahara model at the respective relative humidities using regression analysis with SPSS16.0.

RH	Linear Equation (5)		Quadratic Equation (6)			Cubic Equation (10)			
(%)	R^2	α	R^2	α_1	α_2	R^2	α_1	α_2	α_3
0	0.7568	0.8058	0.9684	−0.5157	0.6315	0.9821	−0.6961	0.8374	0.2698
50	0.7562	0.8050	0.9686	−0.5144	0.6325	0.9821	−0.6932	0.8365	0.2673
70	0.7559	0.8047	0.9687	−0.5139	0.6329	0.9821	−0.6921	0.8362	0.2665
80	0.7557	0.8043	0.9688	−0.5134	0.6332	0.9822	−0.6912	0.8360	0.2659
90	0.7551	0.8036	0.9689	−0.5124	0.6340	0.9822	−0.6896	0.8361	0.2650
95	0.7541	0.8025	0.9690	−0.5108	0.6350	0.9822	−0.6875	0.8366	0.2643
98	0.7519	0.8003	0.9690	−0.5074	0.6375	0.9823	−0.6843	0.8392	0.2645
99	0.7497	0.7979	0.9689	−0.5040	0.6397	0.9824	−0.6816	0.8422	0.2655

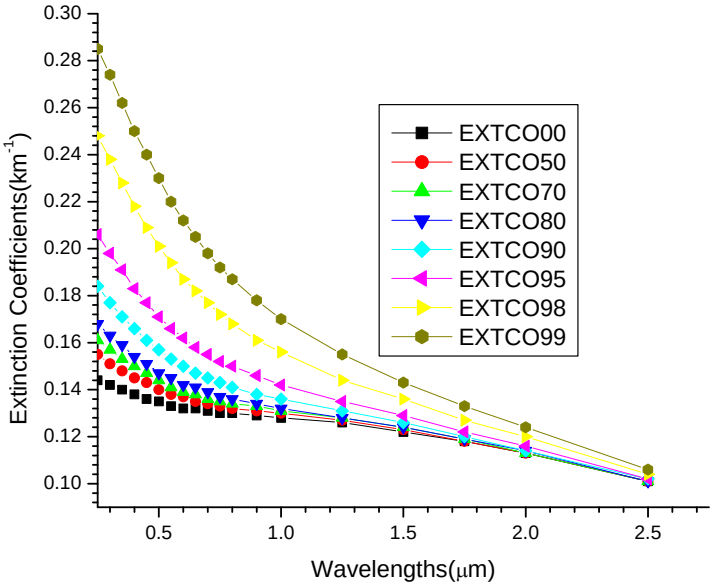

Figure 1(c). A graph of extinction coefficients against wavelength for sahara at RHs 0%, 50%, 70%, 80%, 90%, 95%, 98% and 99%.

Table 2(c). The results of the Angstrom coefficients of extinction coefficients using Equations (5), (6) and (10) for sahara model at the respective relative humidities using regression analysis with SPSS16.0.

RH	Linear Equation (5)		Quadratic Equation (6)			Cubic Equation (10)			
(%)	R^2	α	R^2	α_1	α_2	R^2	α_1	α_2	α_3
0	0.8824	0.1225	0.9422	−0.1442	−0.0473	0.9880	−0.0979	−0.1001	−0.0693
50	0.9411	0.1552	0.9624	−0.1711	−0.0346	0.9911	−0.1261	−0.0859	−0.0673
70	0.9583	0.1733	0.9706	−0.1867	−0.0291	0.9922	−0.1435	−0.0784	−0.0646
80	0.9697	0.1918	0.9770	−0.2031	−0.0247	0.9932	−0.1620	−0.0716	−0.0615
90	0.9836	0.2320	0.9864	−0.2404	−0.0182	0.9948	−0.2047	−0.0588	−0.0533
95	0.9916	0.2855	0.9932	−0.2933	−0.0169	0.9963	−0.2670	−0.0469	−0.0393
98	0.9942	0.3684	0.9974	−0.3827	−0.0310	0.9977	−0.3722	−0.0430	−0.0156
99	0.9914	0.4272	0.9985	−0.4517	−0.0535	0.9985	−0.4520	−0.0532	0.0004

Table 2(d). The results of the Angstrom coefficients of extinction coefficients using Equations (1), (7), (9) and (12) for sahara model at the respective relative humidities using regression analysis with SPSS16.0.

RH	Linear		Quadratic		Cubic	
(%)	Equation (7)	Equation (1)	Equation (9)	Equation (1)	Equation (12)	Equation (1)
	A	A	α_1 (λ)	α_1 (λ)	α_2 (λ)	α_2 (λ)
0	0.122451	0.101199	0.115492	0.159794	0.139420	0.141914
50	0.155226	0.136194	0.150135	0.189424	0.173392	0.175070
70	0.173292	0.155676	0.169010	0.206057	0.191334	0.192991
80	0.191773	0.175054	0.188141	0.222690	0.209395	0.210576
90	0.231990	0.217366	0.229310	0.259265	0.247712	0.248438
95	0.285518	0.273175	0.283026	0.307763	0.296618	0.296840
98	0.368436	0.359011	0.363871	0.382144	0.369275	0.368879
99	0.427181	0.419607	0.419313	0.433753	0.419175	0.418214

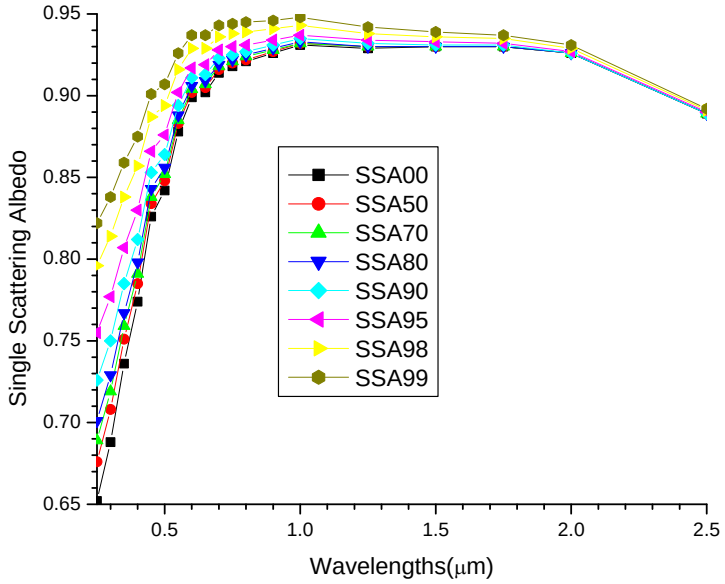

Figure 1(d). A graph of single scattering albedo against wavelength for sahara at RHs 0%, 50%, 70%, 80%, 90%, 95%, 98% and 99%.

Table 2(e). The results of the Angstrom coefficients of single scattering albedo using Equations (5), (6) and (10) for sahara model at the respective relative humidities using regression analysis with SPSS16.0.

RH	Linear Equation (5)		Quadratic Equation (6)			Cubic Equation (10)			
(%)	R^2	α	R^2	α_1	α_2	R^2	α_1	α_2	α_3
0	0.6130	−0.1325	0.9840	0.0623	−0.1529	0.9873	0.0463	−0.1346	0.0239
50	0.6085	−0.1197	0.9840	0.0556	−0.1393	0.9859	0.0446	−0.1268	0.0165
70	0.6044	−0.1129	0.9838	0.0520	−0.1326	0.9851	0.0433	−0.1226	0.0130
80	0.5993	−0.1064	0.9835	0.0484	−0.1263	0.9844	0.0416	−0.1186	0.0102
90	0.5838	−0.0931	0.9828	0.0407	−0.1141	0.9830	0.0373	−0.1103	0.0051
95	0.5534	−0.0773	0.9814	0.0310	−0.1008	0.9814	0.0307	−0.1005	0.0001
98	0.4796	−0.0561	0.9787	0.0171	−0.0848	0.9791	0.0197	−0.0878	−0.0039
99	0.4041	−0.0430	0.9763	0.0082	−0.0758	0.9775	0.0121	−0.0803	−0.0059

Table 2(f). The results of the Angstrom coefficients of single scattering albedo using Equation (2) for sahara model at the respective relative humidities

RH	Linear	Quadratic		Cubic		
(%)	A	α_1	α_2	α_1	α_2	α_3
0	−0.132502	0.062268	−0.15288	0.046363	−0.13473	0.023788
50	−0.119753	0.055814	−0.13917	0.044891	−0.12671	0.016337
70	−0.112727	0.051800	−0.13262	0.043217	−0.12283	0.012838
80	−0.106435	0.048374	−0.12638	0.041661	−0.11872	0.01004
90	−0.093124	0.040653	−0.11421	0.037474	−0.11059	0.004755
95	−0.077282	0.030909	−0.10094	0.030828	−0.10085	0.000121
98	−0.056080	0.017218	−0.08459	0.019982	−0.08774	−0.00413
99	−0.043050	0.008194	−0.07587	0.01212	−0.08035	−0.00587

can be observed that they are approximately the same with some to three places of decimal while some to four places of decimals.

Figure 1(e) shows it is almost the opposite of **Figure 1(d)**, and the plots can be barely approximated by power law and it decreases with the increase in RH.

Table 2(g) shows that the correlations decrease with the increase in RH, but increase with the increase in the power of the polynomials.

Comparing the coefficients in **Tables 2(g)** and **(h)** it can be observed that they are approximately the same, some to one place of decimals while some to two places of decimals.

Figure 2(a) shows a steep but smooth decrease of the extinction coefficients with wavelengths and all the plots satisfy power law.

Table 3(a) shows very good correlations for all the polynomials, and the correlations increase with the increase in the powers of the polynomials.

Figure 2(b) shows a steep but smooth curves that decrease with the increase in wavelength, but shows little effect with the increase in RH. They all satisfy power law.

Table 3(b) shows very good correlations for all the polynomials, and the correlations increase with the increase in the powers of the polynomials.

Figures 2(c) and **(a)** are almost similar.

Table 3(c) shows very good correlations for all the equations, but the correlation increases with the increase in the power of the polynomials.

From **Table 3(d)** it can be seen that they are approximately the same, with some to one place of decimal while some to two places of decimals.

Figure 2(d) shows that not all can satisfy power law.

Table 3(e) shows that the correlations decrease with the increase in RH, but increase with the increase in the power of the polynomials.

Comparing the coefficients in **Tables 3(e)** and **(f)** it can be observed that they are approximately the same with some to two places of decimals while some to four places of decimals.

Figure 2(e) is almost the inverse of **Figure 2(d)**.

Table 3(g) shows very good correlations between, and the correlation increases with the increase in the power of the polynomials.

Comparing **Tables 3(g)** and **(h)**, the linear part shows that at 0%, 50% and 70% RH, they are the same to one place of decimal places. After that they are completely different.

Comparing **Figures 3(a)** and **2(a)** it can be observed that they are similar.

Table 4(a) shows very good correlations for all the polynomials, and the correlations increase with the increase in the powers of the polynomials.

From **Figure 3(b)**, the plots barely obey power law.

Table 4(b) shows that the correlations decrease with the increase in RH, but increase with the increase in the power of the polynomials.

Comparing **Figures 3(c)** and **2(c)** it can be observed that they are similar.

Table 4(c) shows very good correlations, and the correlations increases with the increase in the power of the polynomials.

From **Table 4(d)** it can be seen that the coefficients are approximately the same to one place of decimal and some to two places of decimals.

Figure 3(d) shows that power law is not obeyed.

Table 4(e) shows that there are poor correlations in the linear part, but the correlation improves with the increase in the power of the polynomials.

Comparing the coefficients of **Tables 4(e)** and **(f)** it can be observed that they are all approximately the same within two places of decimals, while some to four places of decimals.

Figure 3(e), is the inverse of **Figure 3(d)** and the power law is not obeyed.

Table 4(g) shows that there are poor correlations in the linear part, but the correlation improves with the increase in the power of the polynomials.

Comparing the coefficients of **Tables 4(g)** and **(h)** it

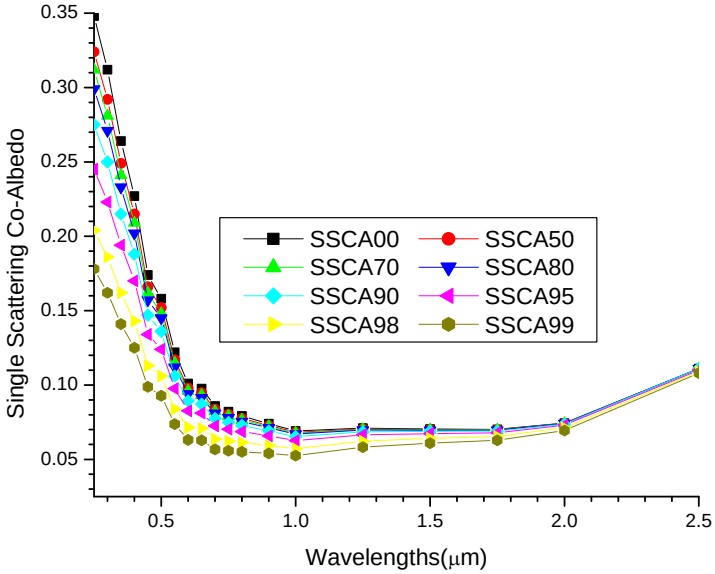

Figure 1(e). A graph of single scattering co-albedo against wavelength for sahara at RHs 0%, 50%, 70%, 80%, 90%, 95%, 98% and 99%.

Table 2(g). The results of the Angstrom coefficients of single scattering co-albedo using Equations (5), (6) and (10) for sahara model at the respective relative humidities using regression analysis with SPSS16.0.

RH	Linear Equation (5)		Quadratic Equation (6)			Cubic Equation (10)			
(%)	R^2	α	R^2	α_1	α_2	R^2	α_1	α_2	α_3
0	0.6604	0.6854	0.9563	−0.3730	0.6800	0.9820	−0.5976	0.9363	0.3359
50	0.6450	0.6510	0.9521	−0.3451	0.6658	0.9803	−0.5714	0.9240	0.3385
70	0.6342	0.6308	0.9511	−0.3271	0.6610	0.9795	−0.5488	0.9139	0.3315
80	0.6242	0.6101	0.9499	−0.3100	0.6532	0.9787	−0.5278	0.9018	0.3258
90	0.5946	0.5710	0.9481	−0.2711	0.6527	0.9774	−0.4818	0.8930	0.3151
95	0.5480	0.5172	0.9427	−0.2183	0.6507	0.9743	−0.4247	0.8863	0.3088
98	0.4483	0.4324	0.9379	−0.1246	0.6699	0.9695	−0.3150	0.8871	0.2848
99	0.3625	0.3721	0.9352	−0.0536	0.6932	0.9654	−0.2319	0.8966	0.2666

Table 2(h). The results of the Angstrom coefficients of single scattering co-albedo using Equation (3) for sahara model at the respective relative humidities.

RH	Linear	Quadratic		Cubic		
(%)	α	α_1	α_2	α_1	α_2	α_3
0	0.68333	−0.37147	0.678817	−0.59818	0.937478	0.339073
50	0.64979	−0.3433	0.667123	−0.56704	0.922397	0.334632
70	0.631366	−0.32723	0.662004	−0.54863	0.914611	0.331136
80	0.61253	−0.3103	0.657862	−0.52921	0.907625	0.327408
90	0.571652	−0.27204	0.652168	−0.48483	0.894952	0.31826
95	0.51703	−0.21752	0.65193	−0.42055	0.883569	0.30365
98	0.431835	−0.12473	0.668464	−0.31204	0.882169	0.280141
99	0.370726	−0.0523	0.693104	−0.22958	0.895362	0.265135

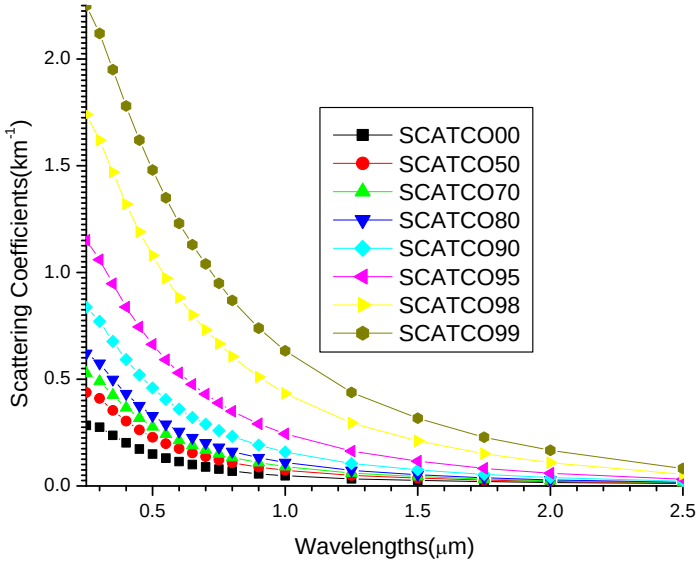

Figure 2(a). A graph of scattering coefficients against wavelength for urban at RHs 0%, 50%, 70%, 80%, 90%, 95%, 98% and 99%.

Table 3(a). The results of the Angstrom coefficients of scattering coefficients using Equations (5), (6) and (10) for urban model at the respective relative humidities using regression analysis with SPSS16.0.

RH	Linear Equation (5)		Quadratic Equation (6)			Cubic Equation (10)			
(%)	R^2	α	R^2	α_1	α_2	R^2	α_1	α_2	α_3
0	0.9906	1.5018	0.9961	−1.5781	−0.1661	0.9993	−1.7201	−0.0041	0.2124
50	0.9853	1.5793	0.9986	−1.7040	−0.2714	0.9997	−1.7925	−0.1704	0.1324
70	0.9816	1.5962	0.9992	−1.7416	−0.3165	0.9998	−1.8045	−0.2447	0.0941
80	0.9779	1.6022	0.9995	−1.7647	−0.3537	0.9998	−1.8060	−0.3065	0.0618
90	0.9698	1.5917	0.9997	−1.7820	−0.4143	0.9997	−1.7851	−0.4107	0.0047
95	0.9602	1.5506	0.9995	−1.7641	−0.4648	0.9996	−1.7325	−0.5008	−0.0473
98	0.9469	1.4597	0.9988	−1.6925	−0.5067	0.9995	−1.6291	−0.5791	−0.0948
99	0.9373	1.3840	0.9983	−1.6243	−0.5231	0.9993	−1.5473	−0.6109	−0.1151

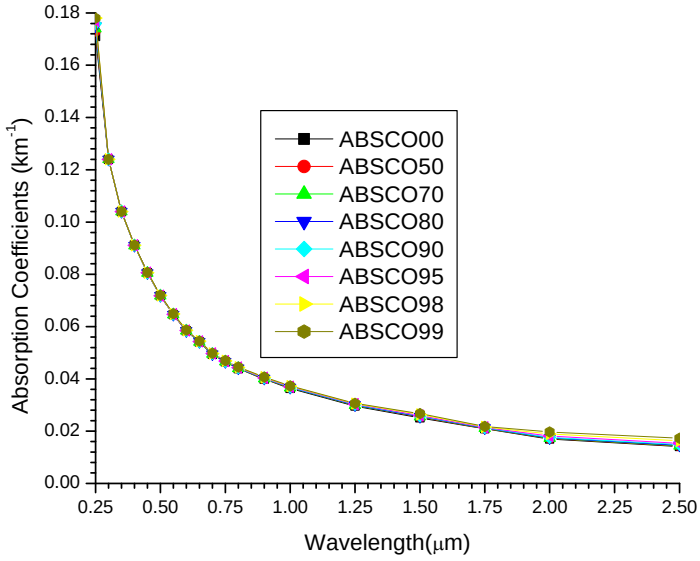

Figure 2(b). A graph of absorption coefficients against wavelength for urban at RHs 0%, 50%, 70%, 80%, 90%, 95%, 98% and 99%.

Table 3(b). The results of the Angstrom coefficients of absorption coefficients using Equations (5), (6) and (10) for urban model at the respective relative humidities using regression analysis with SPSS16.0.

RH	Linear		Quadratic			Cubic			
(%)	R^2	α	R^2	α_1	α_2	R^2	α_1	α_2	α_3
0	0.9958	1.0326	0.9971	−1.0072	0.0554	0.9989	−0.9344	−0.0277	−0.1089
50	0.9951	1.0269	0.9967	−0.9984	0.0620	0.9988	−0.9207	−0.0267	−0.1163
70	0.9948	1.0242	0.9966	−0.9941	0.0655	0.9987	−0.9156	−0.0241	−0.1174
80	0.9945	1.0216	0.9966	−0.9900	0.0688	0.9987	−0.9112	−0.0211	−0.1178
90	0.9940	1.0157	0.9965	−0.9806	0.0763	0.9986	−0.9029	−0.0123	−0.1162
95	0.9932	1.0067	0.9966	−0.9664	0.0877	0.9986	−0.8925	0.0034	−0.1105
98	0.9914	0.9889	0.9970	−0.9385	0.1097	0.9984	−0.8756	0.0380	−0.0940
99	0.9892	0.9716	0.9973	−0.9117	0.1304	0.9982	−0.8618	0.0734	−0.0746

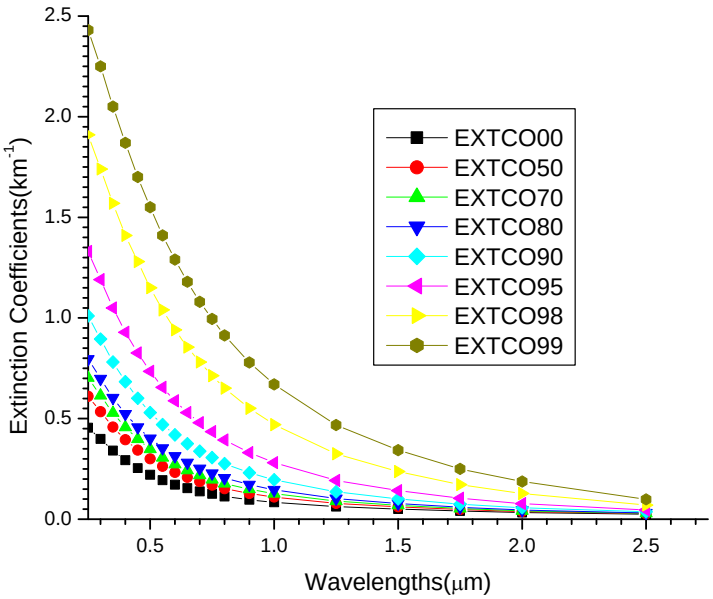

Figure 2(c). A graph of extinction coefficients against wavelength for urban at RHs 0%, 50%, 70%, 80%, 90%, 95%, 98% and 99%.

Table 3(c). The results of the Angstrom coefficients of extinction coefficients using Equations (5), (6) and (10) for urban model at the respective relative humidities using regression analysis with SPSS16.0.

RH	Linear Equation (5)		Quadratic Equation (6)			Cubic Equation (10)			
(%)	R^2	α	R^2	α_1	α_2	R^2	α_1	α_2	α_3
0	0.9975	1.3058	0.9985	−1.3332	−0.0597	0.9995	−1.4040	0.0210	0.1058
50	0.9946	1.3899	0.9991	−1.4535	−0.1384	0.9998	−1.5150	−0.0682	0.0920
70	0.9921	1.4196	0.9993	−1.5021	−0.1795	0.9998	−1.5555	−0.1185	0.0800
80	0.9893	1.4403	0.9995	−1.5402	−0.2176	0.9999	−1.5843	−0.1674	0.0659
90	0.9824	1.4620	0.9998	−1.5947	−0.2889	0.9999	−1.6166	−0.2640	0.0327
95	0.9728	1.4572	0.9999	−1.6229	−0.3607	0.9999	−1.6168	−0.3676	−0.0090
98	0.9579	1.4055	0.9995	−1.6049	−0.4340	0.9998	−1.5647	−0.4799	−0.0601
99	0.9472	1.3480	0.9990	−1.5627	−0.4673	0.9996	−1.5047	−0.5335	−0.0868

Table 3(d). The results of the Angstrom coefficients of extinction coefficients using Equations (1), (7), (9) and (12) for urban model at the respective relative humidities using regression analysis with SPSS16.0.

RH	Linear		Quadratic		Cubic	
(%)	Equation (7)	Equation (1)	Equation (9)	Equation (1)	Equation (12)	Equation (1)
	α	α	$\alpha_1(\lambda)$	$\alpha_1(\lambda)$	$\alpha_2(\lambda)$	$\alpha_2(\lambda)$
0	1.305762	1.317118	1.296971	1.285558	1.260416	1.267717
50	1.389882	1.408679	1.369510	1.351385	1.337729	1.344704
70	1.419598	1.440412	1.393177	1.372674	1.365554	1.371538
80	1.440264	1.462055	1.408237	1.386470	1.385480	1.390167
90	1.461972	1.483500	1.419447	1.397601	1.408146	1.410535
95	1.457184	1.475636	1.404097	1.384973	1.407222	1.407436
98	1.405514	1.418383	1.341632	1.328506	1.362398	1.361215
99	1.348026	1.357473	1.279248	1.269739	1.309238	1.307432

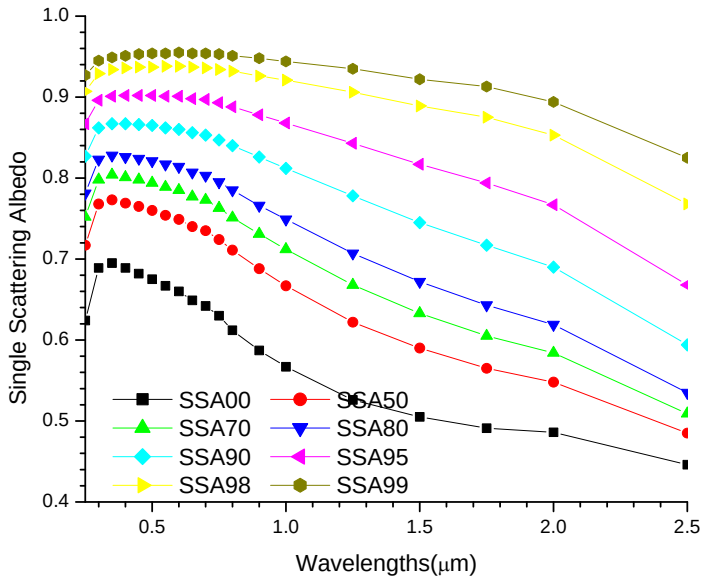

Figure 2(d). A graph of single scattering albedo against wavelength for urban at RHs 0%, 50%, 70%, 80%, 90%, 95%, 98% and 99%.

Table 3(e). The results of the Angstrom coefficients of single scattering albedo using Equations (5), (6) and (10) for urban model at the respective relative humidities using regression analysis with SPSS16.0.

RH	Linear Equation (5)		Quadratic Equation (6)			Cubic Equation (10)			
(%)	R^2	α	R^2	α_1	α_2	R^2	α_1	α_2	α_3
0	0.8376	0.1961	0.9498	−0.2450	−0.1064	0.9898	−0.3162	−0.0252	0.1064
50	0.8070	0.1893	0.9884	−0.2505	−0.1331	0.9942	−0.2772	−0.1026	0.0400
70	0.7798	0.1766	0.9933	−0.2396	−0.1370	0.9942	−0.2491	−0.1261	0.0143
80	0.7515	0.1620	0.9931	−0.2246	−0.1362	0.9932	−0.2216	−0.1396	−0.0044
90	0.6908	0.1297	0.9836	−0.1872	−0.1252	0.9890	−0.1682	−0.1469	−0.0285
95	0.6169	0.0935	0.9637	−0.1412	−0.1039	0.9806	−0.1155	−0.1331	−0.0384
98	0.5108	0.0542	0.9320	−0.0877	−0.0729	0.9656	−0.0646	−0.0993	−0.0345
99	0.4347	0.0359	0.9104	−0.0615	−0.0557	0.9540	−0.0426	−0.0772	−0.0283

Table 3(f). The results of the Angstrom coefficients of single scattering albedo using Equation (2) for urban model at the respective relative humidities.

RH	Linear	Quadratic		Cubic		
(%)	α	α_1	α_2	α_1	α_2	α_3
0	0.196057	−0.244939	−0.106400	−0.316179	−0.025120	0.106549
50	0.189424	−0.250513	−0.132973	−0.277519	−0.102162	0.040390
70	0.176572	−0.239505	−0.136985	−0.248942	−0.126217	0.014115
80	0.161910	−0.224417	−0.136057	−0.221713	−0.139142	−0.004044
90	0.129716	−0.187304	−0.125352	−0.168540	−0.146761	−0.028065
95	0.093392	−0.141213	−0.104091	−0.115660	−0.133245	−0.038218
98	0.054221	−0.087622	−0.072703	−0.064399	−0.099199	−0.034733
99	0.035931	−0.061562	−0.055790	−0.042615	−0.077408	−0.028338

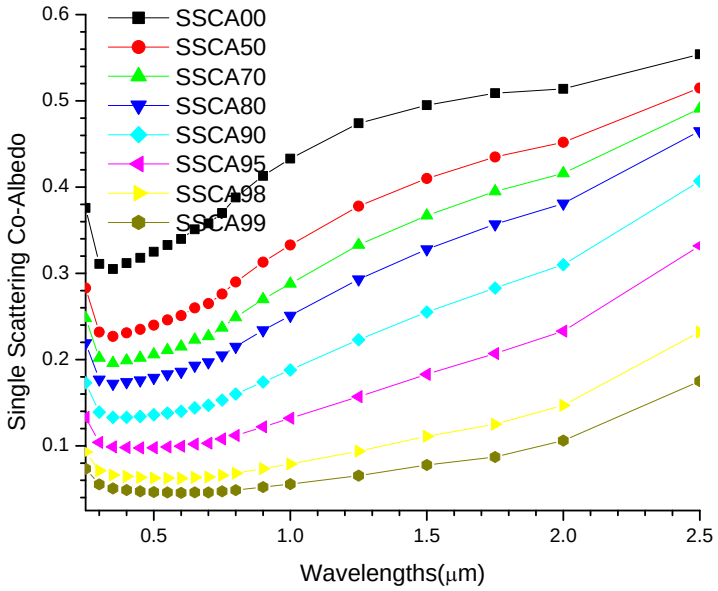

Figure 2(e). A graph of single scattering co-albedo against wavelength for urban at RHs 0%, 50%, 70%, 80%, 90%, 95%, 98% and 99%.

Table 3(g). The results of the Angstrom coefficients of single scattering co-albedo using Equations (5), (6) and (10) for urban model at the respective relative humidities using regression analysis with SPSS16.0.

RH	Linear Equation (5)		Quadratic Equation (6)			Cubic Equation (10)			
(%)	R^2	α	R^2	α_1	α_2	R^2	α_1	α_2	α_3
0	0.8636	−0.2906	0.8981	0.5267	−0.0928	0.9096	0.1643	0.2374	−0.0831
50	0.9171	−0.3964	0.9780	0.5457	−0.0587	0.9425	−0.0459	0.4805	−0.1357
70	0.9291	−0.4395	0.9313	0.5270	−0.0344	0.9508	−0.1609	0.5924	−0.1577
80	0.9327	−0.4714	0.9327	0.4762	−0.0019	0.9548	−0.3073	0.7121	−0.1796
90	0.9258	−0.5157	0.9320	0.3446	0.0673	0.9585	−0.5964	0.9248	−0.2158
95	0.8984	−0.5383	0.9292	0.1331	0.1593	0.9593	−0.9312	1.1292	−0.2440
98	0.8247	−0.5262	0.9197	0.1593	0.2855	0.9562	−1.3954	1.3749	−0.2741
99	0.7478	−0.4986	0.9077	0.2855	0.0695	0.9510	−1.7342	1.5489	−0.2970

Table 3(h). The results of the Angstrom coefficients of single scattering co-albedo using Equation (3) for urban model at the respective relative humidities.

RH	Linear	Quadratic		Cubic		
(%)	α	α_1	α_2	α_1	α_2	α_3
0	−0.273154	0.326035	0.115104	0.469589	−0.048684	−0.214705
50	−0.362993	0.455074	0.200432	0.594301	0.041582	−0.208233
70	−0.395439	0.508002	0.245014	0.639970	0.094445	−0.197376
80	−0.418647	0.550228	0.286412	0.673048	0.146282	−0.183694
90	−0.446297	0.614085	0.365224	0.713632	0.251647	−0.148885
95	−0.450505	0.656495	0.448377	0.724332	0.370979	−0.101459
98	−0.416653	0.666450	0.543730	0.689108	0.517878	−0.033888
99	−0.376471	0.651039	0.597649	0.642886	0.606951	0.012194

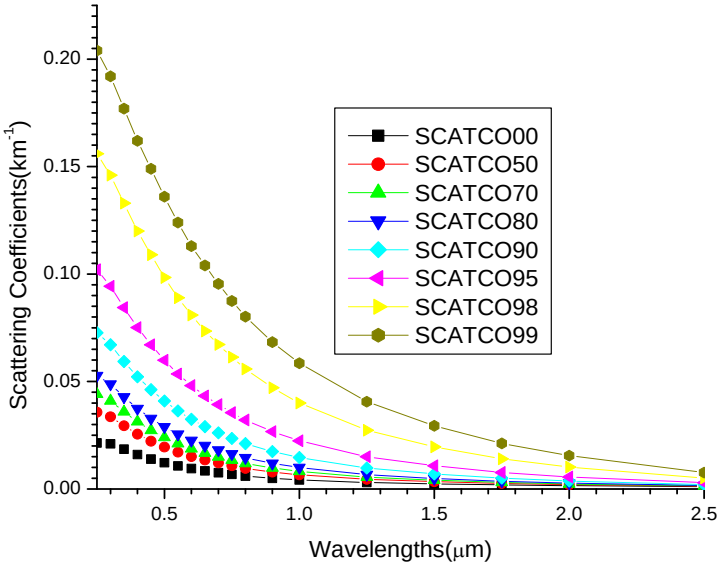

Figure 3(a). A graph of scattering coefficients against wavelength for continental clean at RHs 0%, 50%, 70%, 80%, 90%, 95%, 98% and 99%.

Table 4(a). The results of the Angstrom coefficients of scattering coefficients using Equations (5), (6) and (10) for continental clean model at the respective relative humidities using regression analysis with SPSS16.0.

RH	Linear Equation (5)		Quadratic Equation (6)			Cubic Equation (10)			
(%)	R^2	α	R^2	α_1	α_2	R^2	α_1	α_2	α_3
0	0.9887	1.3858	0.9956	−1.4647	−0.1718	0.9991	−1.6016	−0.0156	0.2048
50	0.9839	1.5029	0.9985	−1.6276	−0.2715	0.9997	−1.7142	−0.1727	0.1295
70	0.9802	1.5327	0.9992	−1.6781	−0.3164	0.9998	−1.7403	−0.2454	0.0931
80	0.9763	1.5483	0.9995	−1.7108	−0.3537	0.9998	−1.7522	−0.3065	0.0619
90	0.9682	1.5522	0.9998	−1.7429	−0.4151	0.9998	−1.7469	−0.4106	0.0060
95	0.9586	1.5227	0.9995	−1.7371	−0.4666	0.9997	−1.7067	−0.5013	−0.0455
98	0.9451	1.4423	0.9988	−1.6764	−0.5096	0.9995	−1.6141	−0.5807	−0.0933
99	0.9356	1.3710	0.9983	−1.6127	−0.5260	0.9993	−1.5366	−0.6129	−0.1138

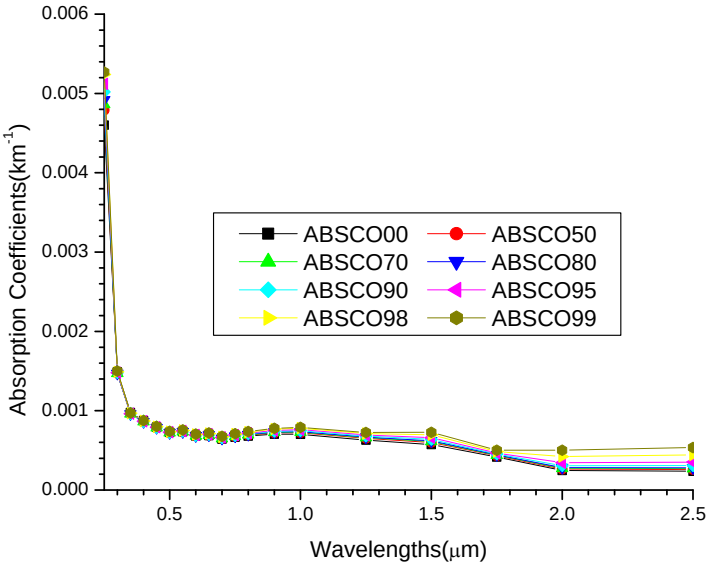

Figure 3(b). A graph of absorption coefficients against wavelength for continental clean at RHs 0%, 50%, 70%, 80%, 90%, 95%, 98% and 99%.

Table 4(b). The results of the Angstrom coefficients of absorption coefficients using Equations (5), (6) and (10) for continental clean model at the respective relative humidities using regression analysis with SPSS16.0.

RH	Linear		Quadratic			Cubic			
(%)	R^2	α	R^2	α_1	α_2	R^2	α_1	α_2	α_3
0	0.7321	0.8145	0.7574	−0.7114	0.2243	0.9472	−0.0227	−0.5615	−1.0300
50	0.6988	0.7801	0.7326	−0.6633	0.2542	0.9397	0.0419	−0.5504	−1.0547
70	0.6866	0.7655	0.7252	−0.6419	0.2690	0.9368	0.0638	−0.5362	−1.0555
80	0.6757	0.7518	0.7195	−0.6214	0.2838	0.9343	0.0824	−0.5193	−1.0527
90	0.6537	0.7228	0.7108	−0.5773	0.3168	0.9293	0.1166	−0.4749	−1.0378
95	0.6226	0.6824	0.7026	−0.5158	0.3626	0.9219	0.1567	−0.4047	−1.0058
98	0.5596	0.6126	0.6940	−0.4082	0.4450	0.9083	0.2214	−0.2733	−0.9416
99	0.4973	0.5532	0.6912	−0.3180	0.5120	0.8954	0.2707	−0.1597	−0.8805

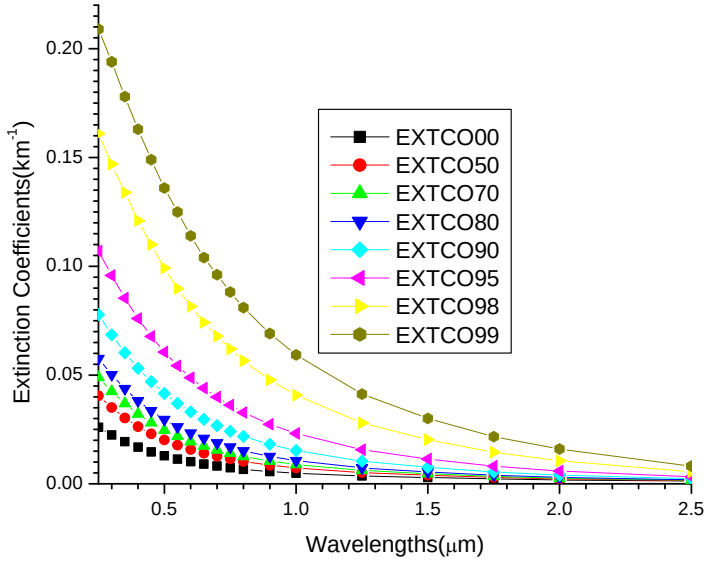

Figure 3(c). A graph of extinction coefficients against wavelength for continental clean at RHs 0%, 50%, 70%, 80%, 90%, 95%, 98% and 99%.

Table 4(c). The results of the Angstrom coefficients of extinction coefficients using Equations (5), (6) and (10) for continental clean model at the respective relative humidities using regression analysis with SPSS16.0.

RH	Linear Equation (5)		Quadratic Equation (6)			Cubic Equation (10)			
(%)	R^2	α	R^2	α_1	α_2	R^2	α_1	α_2	α_3
0	0.9951	1.3264	0.9988	−1.3815	−0.1200	0.9993	−1.4324	−0.0620	0.0761
50	0.9891	1.4450	0.9995	−1.5460	−0.2197	0.9997	−1.5823	−0.1782	0.0544
70	0.9852	1.4790	0.9997	−1.6010	−0.2655	0.9998	−1.6265	−0.2364	0.0381
80	0.9813	1.4991	0.9998	−1.6390	−0.3046	0.9998	−1.6529	−0.2888	0.0207
90	0.9732	1.5122	0.9998	−1.6827	−0.3711	0.9999	−1.6729	−0.3822	−0.0146
95	0.9633	1.4924	0.9996	−1.6898	−0.4295	0.9998	−1.6551	−0.4691	−0.0518
98	0.9495	1.4220	0.9991	−1.6432	−0.4816	0.9997	−1.5828	−0.5505	−0.0903
99	0.9397	1.3554	0.9986	−1.5864	−0.5028	0.9995	−1.5140	−0.5853	−0.1082

Table 4(d). The results of the Angstrom coefficients of extinction coefficients using Equations (1), (7), (9) and (12) for continental clean model at the respective relative humidities using regression analysis with SPSS16.0.

RH	Linear		Quadratic		Cubic	
(%)	Equation (7)	Equation (1)	Equation (9)	Equation (1)	Equation (12)	Equation (1)
	α	α	$\alpha_1(\lambda)$	$\alpha_1(\lambda)$	$\alpha_2(\lambda)$	$\alpha_2(\lambda)$
0	1.326374	1.323762	1.308708	1.288183	1.282407	1.297761
50	1.445043	1.446130	1.412712	1.390209	1.393925	1.411310
70	1.478996	1.481190	1.439914	1.417335	1.426736	1.443978
80	1.499053	1.501993	1.454219	1.432156	1.447062	1.463395
90	1.512202	1.515944	1.457587	1.437578	1.462620	1.476845
95	1.492423	1.496337	1.429202	1.412395	1.447108	1.458491
98	1.421950	1.425678	1.351065	1.338642	1.382278	1.390248
99	1.355396	1.358777	1.281397	1.271155	1.318791	1.324581

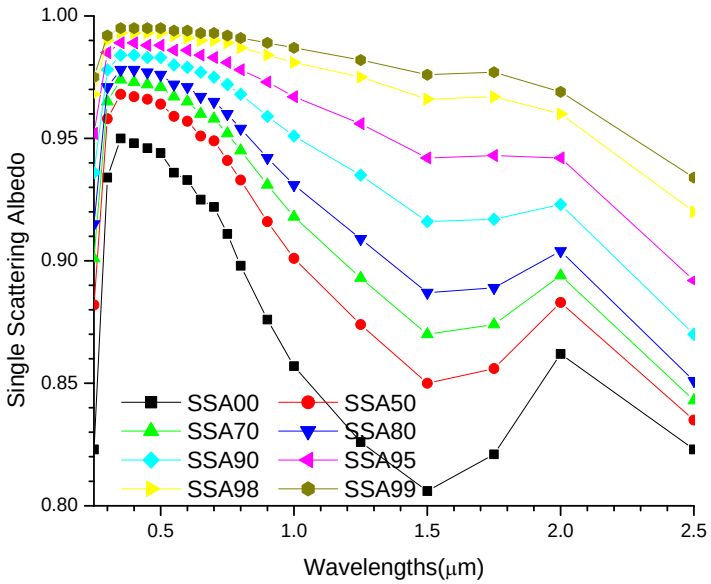

Figure 3(d). A graph of single scattering albedo against wavelength for continental clean at RHs 0%, 50%, 70%, 80%, 90%, 95%, 98% and 99%.

Table 4(e). The results of the Angstrom coefficients of single scattering albedousing Equations (5), (6) and (10) for continental clean model at the respective relative humidities using regression analysis with SPSS16.0.

RH	Linear Equation (5)		Quadratic Equation (6)			Cubic Equation (10)			
(%)	R^2	α	R^2	α_1	α_2	R^2	α_1	α_2	α_3
0	0.4258	0.0592	0.5733	−0.0830	−0.0517	0.8994	−0.1691	0.0465	0.1288
50	0.5636	0.0578	0.7714	−0.0817	−0.0520	0.9251	−0.1318	0.0052	0.0749
70	0.5886	0.0537	0.8283	−0.0771	−0.0508	0.9299	−0.1142	−0.0085	0.0555
80	0.5963	0.0493	0.8647	−0.0718	−0.0490	0.9317	−0.0992	−0.0177	0.0410
90	0.5850	0.0400	0.9057	−0.0602	−0.0439	0.9300	−0.0737	−0.0285	0.0202
95	0.5456	0.0303	0.9168	−0.0472	−0.0370	0.9205	−0.0514	−0.0323	0.0062
98	0.4788	0.0202	0.9037	−0.0331	−0.0281	0.9053	−0.0311	−0.0303	−0.0029
99	0.4350	0.0155	0.8847	−0.0262	−0.0233	0.8939	−0.0224	−0.0276	−0.0056

Table 4(f). The results of the Angstrom coefficients of single scattering albedo using Equations (2) for continental clean model at the respective relative humidities.

RH	Linear	Quadratic		Cubic		
(%)	α	α_1	α_2	α_1	α_2	α_3
0	0.059431	−0.083205	−0.051747	−0.169206	0.046376	0.128627
50	0.057803	−0.081609	−0.051818	−0.131833	0.005485	0.075117
70	0.053680	−0.077069	−0.050912	−0.113828	−0.008971	0.054979
80	0.049226	−0.071792	−0.049118	−0.099330	−0.017699	0.041187
90	0.039996	−0.060241	−0.044067	−0.073978	−0.028393	0.020547
95	0.030288	−0.047315	−0.037062	−0.051545	−0.032235	0.006327
98	0.020366	−0.033218	−0.027974	−0.031264	−0.030203	−0.002922
99	0.015601	−0.026296	−0.023278	−0.022555	−0.027546	−0.005594

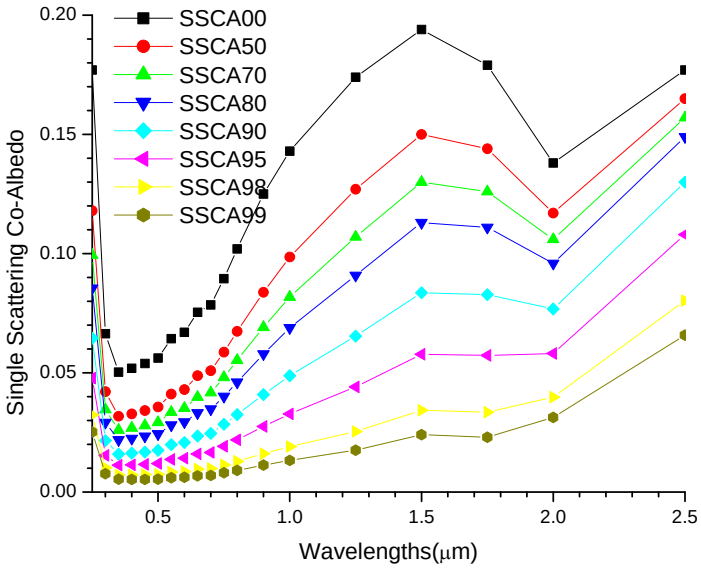

Figure 3(e). A graph of single scattering co-albedo against wavelength for continental clean at RHs 0%, 50%, 70%, 80%, 90%, 95%, 98% and 99%.

Table 4(g). The results of the Angstrom coefficients of single scattering co-albedo using Equations (5), (6) and (10) for continental clean model at the respective relative humidities using regression analysis with SPSS16.0.

RH	Linear Equation (5)		Quadratic Equation (6)			Cubic Equation (10)			
(%)	R^2	α	R^2	α_1	α_2	R^2	α_1	α_2	α_3
0	0.4639	−0.5115	0.5585	0.6689	0.3425	0.9093	1.4075	−0.5003	−1.1048
50	0.5534	−0.6649	0.6829	0.8839	0.4767	0.9333	1.6267	−0.3708	−1.1109
70	0.5742	−0.7143	0.7200	0.9595	0.5337	0.9386	1.6912	−0.3012	−1.0944
80	0.5820	−0.7472	0.7475	1.0186	0.5907	0.9425	1.7369	−0.2289	−1.0743
90	0.5831	−0.7899	0.7850	1.1065	0.6890	0.9438	1.7909	−0.0918	−1.0236
95	0.5671	−0.8087	0.8147	1.1726	0.7921	0.9433	1.8121	0.0625	−0.9564
98	0.5308	−0.8104	0.8471	1.2365	0.9275	0.9419	1.8051	0.2788	−0.8504
99	0.5013	−0.8068	0.8635	1.2738	1.0165	0.9396	1.7958	0.4209	−0.7808

Table 4(h). The results of the Angstrom coefficients of single scattering co-albedo using Equation (3) for continental clean model at the respective relative humidities.

RH	Linear	Quadratic		Cubic		
(%)	α	α_1	α_2	α_1	α_2	α_3
0	−0.511894	0.670076	0.344312	1.409672	−0.499528	−1.106169
50	−0.664984	0.882661	0.473817	1.624198	−0.372238	−1.109071
70	−0.713497	0.959074	0.534546	1.690289	−0.299732	−1.093633
80	−0.747241	1.017557	0.588393	1.735258	−0.230466	−1.073422
90	−0.789407	1.105397	0.687812	1.789529	−0.092746	−1.023214
95	−0.810037	1.173939	0.792101	1.811768	0.064371	−0.953962
98	−0.809353	1.235052	0.926614	1.804207	0.277238	−0.851250
99	−0.802192	1.268369	1.014724	1.784694	0.425625	−0.772235

can be observed that they are approximately the same within two places of decimals, with some to three places of decimals.

Figure 4(a) shows that power law decreases with the increase in RHs.

From **Table 5(a)**, it can be observe that the correlations decrease with the increase in RHs, but increases with the increase in the power of the polynomials.

From **Figure 4(b)** it can be observed that power law is not obeyed.

Table 5(b) shows poor correlation in the linear part, but good correlations at second and third order polynomials, and the correlations increase with the increase in order of the polynomials and RHs.

Comparing **Figures 4(c)** and **(a)**, it can be observed that they are similar.

From **Table 5(c)**, it can be seen that the correlations decrease with the increase in RHs, but increases with the increase in the power of the polynomials.

From **Table 5(d)**, from the linear part it can be seen that Equation (1) underestimated Equation (7) at 0% to 70% RH, and overestimated it at 90% to 99% RH. At the quadratic part Equations (1) and (9) are equal within two places of decimals, but at RHs 95% to 99% Equation (1) underestimated Equation (9). At the cubic part, Equations (1) and (12) are the same within two places of decimals except at 98% and 99% where Equation (1) underestimated Equation (2).

Figure 4(d) shows that power law is not obeyed.

From **Table 5(e)** it can be seen from the linear part that there is a poor correlation between single scattering albedo and wavelength, though as the power of the polynomials increase the relation also improves.

Comparing **Tables 5(e)** and **(f)** it can be observed that in the linear part only the values at 80%, 95% and 99% agree to three places of decimals. This can be attributed to the poor correlations at **Table 5(e)**. From the quadratic and cubic some coefficients agree to two places while some to three places of decimals.

Figure 4(e) in the inverse of **Figure 4(d**).

Table 5(g) shows poor correlations in the linear part. There are good correlations at quadratic and cubic polynomials, though poor correlation can be observed at 99% RH throughout.

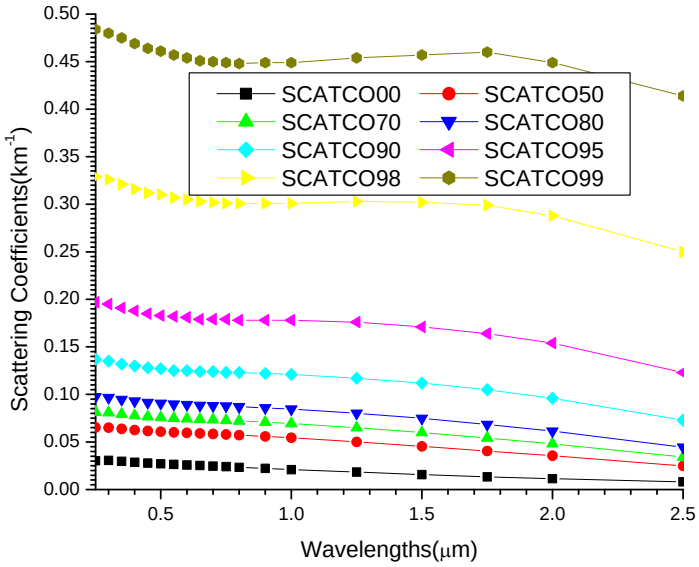

Figure 4(a). A graph of scattering coefficients against wavelength for maritime clean at RHs 0%, 50%, 70%, 80%, 90%, 95%, 98% and 99%.

Table 5(a). The results of the Angstrom coefficients of scattering coefficients using Equations (5), (6) and (10) for maritime clean model at the respective relative humidities using regression analysis with SPSS16.0.

RH	Linear Equation (5)		Quadratic Equation (6)			Cubic Equation (10)			
(%)	R^2	α	R^2	α_1	α_2	R^2	α_1	α_2	α_3
0	0.8698	0.5242	0.9906	−0.6572	−0.2896	0.9989	−0.5721	−0.3867	−0.1273
50	0.7704	0.3328	0.9539	−0.4434	−0.2408	0.9946	−0.3163	−0.3858	−0.1901
70	0.7525	0.2866	0.9366	−0.3832	−0.2102	0.9915	−0.2546	−0.3568	−0.1922
80	0.7397	0.2515	0.9199	−0.3360	−0.1841	0.9883	−0.2091	−0.3289	−0.1899
90	0.7244	0.1908	0.8796	−0.2510	−0.1310	0.9784	−0.1340	−0.2645	−0.1750
95	0.7060	0.1340	0.8192	−0.1706	−0.0796	0.9554	−0.0728	−0.1911	−0.1462
98	0.6908	0.0730	0.7125	−0.0818	−0.0192	0.8845	−0.0213	−0.0882	−0.0905
99	0.6084	0.0401	0.6268	−0.0353	0.0103	0.7891	−9.5139	−0.0289	−0.0514

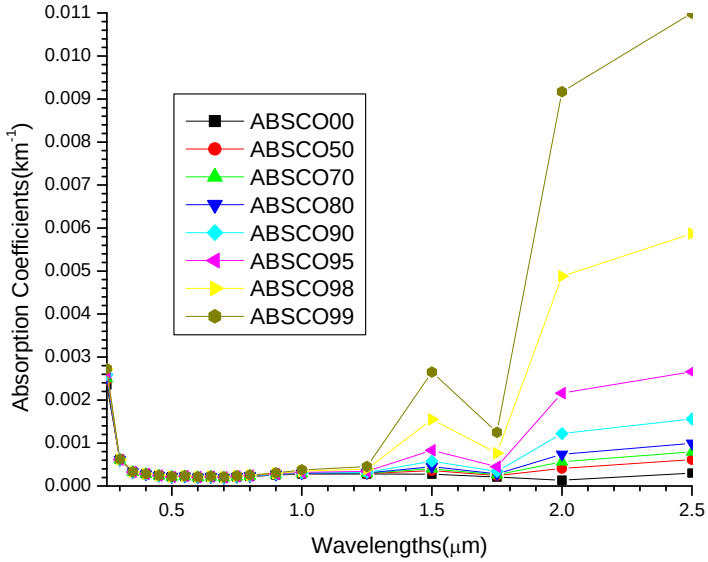

Figure 4(b). A graph of absorption coefficients against wavelength for maritime clean at RHs 0%, 50%, 70%, 80%, 90%, 95%, 98% and 99%.

Table 5(b). The results of the Angstrom coefficients of absorption coefficients using Equations (5), (6) and (10) for maritime clean model at the respective relative humidities using regression analysis with SPSS16.0.

RH	Linear		Quadratic			Cubic			
(%)	R^2	α	R^2	α_1	α_2	R^2	α_1	α_2	α_3
0	0.2846	0.4908	0.6576	−0.1081	0.8328	0.8516	0.5647	0.0652	−1.0063
50	0.0391	0.1833	0.7554	0.3512	1.1634	0.8894	0.9147	0.5204	−0.8429
70	0.0067	0.0799	0.7822	0.5037	1.2703	0.8899	1.0339	0.6653	−0.7930
80	0.0001	−0.0106	0.8041	0.6368	1.3629	0.8903	1.1369	0.7923	−0.7480
90	0.0277	−0.1927	0.8392	0.9028	1.5455	0.8943	1.3540	1.0307	−0.6748
95	0.0961	−0.4180	0.8720	1.2267	1.7603	0.9050	1.6339	1.2957	−0.6090
98	0.2118	−0.7747	0.9045	1.7287	2.0765	0.9230	2.1088	1.6428	−0.5686
99	0.2933	−1.0722	0.9205	2.1399	2.3242	0.9338	2.5189	1.8917	−0.5669

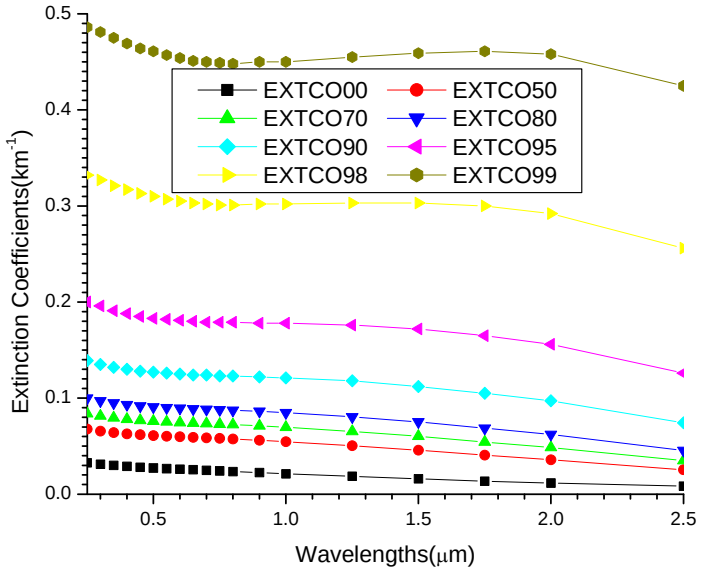

Figure 4(c). A graph of extinction coefficients against wavelength for maritime clean at RHs 0%, 50%, 70%, 80%, 90%, 95%, 98% and 99%.

Table 5(c). The results of the Angstrom coefficients of extinction coefficients using Equations (5), (6) and (10) for maritime clean model at the respective relative humidities using regression analysis with SPSS16.0.

RH	Linear		Quadratic			Cubic			
(%)	R^2	α	R^2	α_1	α_2	R^2	α_1	α_2	α_3
0	0.8883	0.5272	0.9880	−0.6475	−0.2618	0.9998	−0.5464	−0.3772	−0.1512
50	0.7887	0.3333	0.9515	−0.4365	−0.2245	0.9966	−0.3041	−0.3755	−0.1980
70	0.7704	0.2863	0.9352	−0.3765	−0.1963	0.9942	−0.2449	−0.3464	−0.1968
80	0.7571	0.2501	0.9180	−0.3286	−0.1709	0.9910	−0.1997	−0.3180	−0.1928
90	0.7395	0.1877	0.8798	−0.2434	−0.1212	0.9817	−0.1277	−0.2533	−0.1731
95	0.7260	0.1300	0.8153	−0.1611	−0.0676	0.9608	−0.0644	−0.1778	−0.1445
98	0.7056	0.0686	0.7108	−0.0726	−0.0088	0.8872	−0.0157	−0.0737	−0.0852
99	0.5279	0.0332	0.6218	−0.0236	0.0207	0.7764	0.0062	−0.0133	−0.0446

Table 5(d). The results of the Angstrom coefficients of extinction coefficients using Equations (1), (7), (9) and (12) for maritime clean model at the respective relative humidities using regression analysis with SPSS16.0.

RH	Linear		Quadratic		Cubic	
(%)	Equation (7)	Equation (1)	Equation (9)	Equation (1)	Equation (12)	Equation (1)
	α	α	$\alpha_1(\lambda)$	$\alpha_1(\lambda)$	$\alpha_2(\lambda)$	$\alpha_2(\lambda)$
0	0.527214	0.508211	0.488677	0.486895	0.540925	0.548030
50	0.333319	0.328780	0.300276	0.298072	0.368672	0.371082
70	0.286304	0.284118	0.257418	0.254929	0.325406	0.327440
80	0.250051	0.250105	0.224894	0.222541	0.291486	0.293302
90	0.187726	0.190850	0.169883	0.167824	0.229678	0.232161
95	0.130000	0.135132	0.120053	0.115855	0.169988	0.169726
98	0.068600	0.075620	0.067313	0.059593	0.096742	0.094223
99	0.033156	0.043773	0.036207	0.026458	0.051601	0.048180

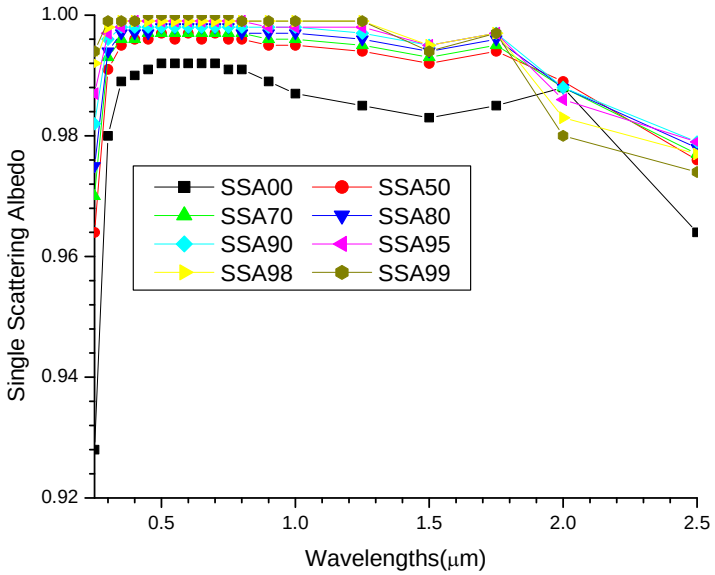

Figure 4(d). A graph of single scattering albedo against wavelength for maritime clean at RHs 0%, 50%, 70%, 80%, 90%, 95%, 98% and 99%.

Table 5(e). The results of the Angstrom coefficients of single scattering albedo using Equations (4), (5) and (6) for maritime clean model at the respective relative humidities using regression analysis with SPSS16.0.

RH	Linear		Quadratic			Cubic			
(%)	R^2	α	R^2	α_1	α_2	R^2	α_1	α_2	α_3
0	0.0260	−0.0039	0.5943	−0.0085	−0.0271	0.7281	−0.0233	−0.0103	0.0220
50	0.0004	0.0003	0.6761	−0.0071	−0.0159	0.7296	−0.0121	−0.0102	0.0075
70	0.0035	0.0007	0.7124	−0.0073	−0.0144	0.7396	−0.0105	−0.0108	0.0047
80	0.0165	0.0013	0.7493	−0.0074	−0.0133	0.7614	−0.0093	−0.0111	0.0029
90	0.0684	0.0023	0.7647	−0.0074	−0.0110	0.7650	−0.0071	−0.0113	−0.0004
95	0.1733	0.0036	0.8283	−0.0085	−0.0105	0.8358	−0.0072	−0.0119	−0.0019
98	0.2977	0.0052	0.8145	−0.0098	−0.0101	0.8683	−0.0062	−0.0143	−0.0055
99	0.3691	0.0068	0.8278	−0.0119	−0.0112	0.8850	−0.0075	−0.0162	−0.0066

Table 5(f). The results of the Angstrom coefficients of single scattering albedo using equations (2) for maritime clean model at the respective relative humidities.

RH	Linear	Quadratic		Cubic		
(%)	α	α_1	α_2	α_1	α_2	α_3
0	−0.003031	−0.009733	−0.027784	−0.025744	−0.009515	0.023948
50	−0.000519	−0.006946	−0.016250	−0.012226	−0.010226	0.007896
70	0.000302	−0.006685	−0.013895	−0.009724	−0.010429	0.004544
80	0.001435	−0.007465	−0.013124	−0.009357	−0.010965	0.002831
90	0.003115	−0.007588	−0.009736	−0.006272	−0.011237	−0.001968
95	0.003996	−0.009503	−0.011988	−0.008400	−0.013246	−0.001649
98	0.004397	−0.009176	−0.010401	−0.005641	−0.014434	−0.005286
99	0.006924	−0.011701	−0.010399	−0.007112	−0.015636	−0.006865

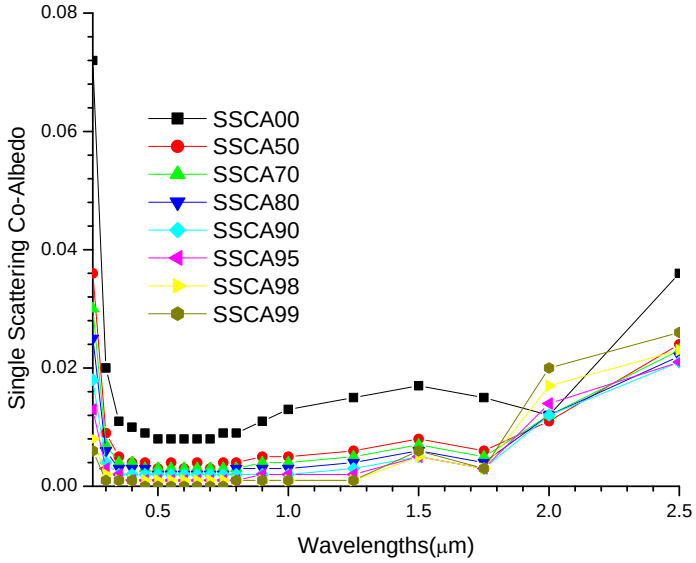

Figure 4(e). A graph of single scattering co-albedo against wavelength for maritime clean at RHs 0%, 50%, 70%, 80%, 90%, 95%, 98% and 99%.

Table 5(g). The results of the Angstrom coefficients of single scattering co-albedo using Equations (5), (6) and (10) for maritime clean model at the respective relative humidities using regression analysis with SPSS16.0.

RH	Linear Equation (5)		Quadratic Equation (6)			Cubic Equation (10)			
(%)	R^2	α	R^2	α_1	α_2	R^2	α_1	α_2	α_3
0	0.0012	−0.0302	0.7001	0.5346	1.0978	0.8425	1.0898	0.4644	−0.8304
50	0.0257	−0.1670	0.8072	0.7943	1.3654	0.8798	1.2605	0.8335	−0.6973
70	0.0417	−0.2199	0.8484	0.8785	1.4336	0.8947	1.2634	0.9944	−0.5757
80	0.0575	−0.2906	0.8604	1.0301	1.6097	0.9018	1.4397	1.1424	−0.6126
90	0.0964	−0.3763	0.8397	1.0881	1.5493	0.8530	1.3202	1.2845	−0.3472
95	0.1709	−0.6389	0.8835	1.5274	1.9340	0.9221	2.0316	1.3586	−0.7542
98	0.2308	−0.7704	0.8858	1.6544	1.9240	0.8870	1.7469	1.8184	−0.1384
99	0.1270	−0.5957	0.2027	0.9088	0.6816	0.3329	−0.0929	1.8245	1.4982

Comparing **Tables 5(g)** and **(h)** it can be seen that from the linear part they are different, and this can be attributed to the poor correlations in **5(g)**. From the quadratic and cubic, the coefficients from **Tables 5(g)** and **(h)**

Table 5(h). The results of the Angstrom coefficients of single scattering co-albedo using Equation (3) for maritime clean model at the respective relative humidities.

RH	Linear	Quadratic		Cubic		
(%)	α	α_1	α_2	α_1	α_2	α_3
0	−0.036462	0.539358	1.094649	−0.018294	0.312034	1.157534
50	−0.150011	0.787625	1.387888	−0.610640	−0.144866	1.040860
70	−0.206397	0.880150	1.466550	−0.789011	−0.318965	0.989806
80	−0.260667	0.965345	1.533866	−0.937193	−0.474357	0.940760
90	−0.380442	1.146174	1.666761	−1.226255	−0.777471	0.847912
95	−0.548017	1.387765	1.827872	−1.569516	−1.117854	0.753569
98	−0.843281	1.801288	2.085286	−2.093174	−1.569053	0.653780
99	−1.105303	2.163529	2.303430	−2.525064	−1.878473	0.611415

are almost the same, but to only one place of decimals.

4. Conclusions

From all the tables and graphs obtained, it can be seen that it is only urban aerosols that scattering, absorption and extinction coefficients that satisfy power laws excellently at this spectral range and can be seen that it is the only aerosols that show very good relations between the estimated Equations (1)-(3) and the linear Equation (5). Linear models are considered most important, because they are the values that are obtainable from remote sensing and ground truthing instruments.

Another observation made is that Equations (1) and (2) are sufficient. This is because the information that can be obtained from equation is almost the same as that of Equation (3).

Additional important observation made from the various graphs is that, at the spectral range of 0.4 to 1.5 power laws are obeyed by all the aerosols. Therefore, since 99% of sun's radiation falls between 0.2 - 5.6 μm; and 80% falls between 0.4 - 1.5 μm (visible and near infrared) and the atmosphere is quite transparent to incoming solar radiation with the maximum radiation at 0.48 μm (visible) and in the study of the earth's surface, most of the remote sensing instruments are designed to operate within solar spectral window (0.4 - 0.7 μm) and near infrared (0.7 - 1.5 μm), where cloudless atmosphere will transmit sufficient radiation for detection, which also shows that these formulas can be useful in remote sensing.

REFERENCES

[1] A. Angstrom, "On the Atmospheric Transmission of Sun Radiation and on Dust in the Air," *Geografiska Annaler*, Vol. 11, 1929, pp. 156-166. http://dx.doi.org/10.2307/519399

[2] A. Angstrom, "On the Atmospheric Transmission of Sun Radiation II," *Geografiska Annaler*, Vol. 12, 1930, pp. 130-159. http://dx.doi.org/10.2307/519561

[3] A. Angstrom, "Techniques of Determining the Turbidity of the Atmosphere," *Tellus*, Vol. 13, No. 2, 1961, pp. 214-223. http://dx.doi.org/10.1111/j.2153-3490.1961.tb00078.x

[4] A. Angstrom, "The Parameters of Atmospheric Turbidity," *Tellus*, Vol. 16, No. 1, 1964, pp. 64-75. http://dx.doi.org/10.1111/j.2153-3490.1964.tb00144.x

[5] P. B. Russell, R. W. Bergstrom, Y. Shinozuka, A. D. Clarke, P. F. De-Carlo, J. L. Jimenez, J. M. Livingston, J. Redemann, O. Dubovik and A. Strawa, "Absorption Angstrom Exponent in AERONET and Related Data as an Indicator of Aerosol Composition," *Atmospheric Chemistry and Physics*, Vol. 10, 2010, pp. 1155-1169. http://dx.doi.org/10.5194/acp-10-1155-2010

[6] E. V. Fischer, D. A. Jaffe, N. A. Marley, J. S. Gaffney and A. Marchany-Rivera, "Optical Properties of Aged Asian Aerosols Observed over the US Pacific Northwest," *Journal of Geophysical Research*, Vol. 115, No. D20, 2010. http://dx.doi.org/10.1029/2010JD013943

[7] A. Virkkula, N. C. Ahlquist, D. S. Covert, W. P. Arnott, P. J. Sheridan, P. K. Quinn and D. J. Coffman, "Modification, Calibration and a Field Test of an Instrument for Measuring Light Absorption by Particles," *Aerosol Science and Technology*, Vol. 39, No. 1, 2005, pp. 68-83.

[8] B. A. Flowers, M. K. Dubey, C. Mazzoleni, E. A. Stone, J. J. Schauer, S.-W. Kim and S. C. Yoon, "Optical-Chemical-Microphysical Relationships and Closure Studies for Mixed Car-Bonaceous Aerosols Observed at Jeju Island; 3-Laser Photoa-Coustic Spectrometer, Particle Sizing, and Filter Analysis," *Atmospheric Chemistry and Physics*, Vol. 10, 2010, pp. 10387-10398. http://dx.doi.org/10.5194/acp-10-10387-2010

[9] N. O'Neill and A. Royer, "Extraction of Bimodal Aerosol-Size Distribution Radii from Spectral and Angular Slope (Angstrom) Coefficients," *Applied Optics*, Vol. 32, No. 9, 1993, pp. 1642-1645. http://dx.doi.org/10.1364/AO.32.001642

[10] M. K. Latha and K. V. S. Badarinath, "Factors Influencing Aerosol Characteristics over Urban Environment," *Environmental Monitoring and Assessment*, Vol. 104, No. 1-3, 2005, pp. 269-280. http://dx.doi.org/10.1007/s10661-005-1615-7

[11] J. S. Reid, T. F. Eck, S. A. Christopher, P. V. Hobbs and B. Holben, "Use of the Angstrom Exponent to Estimate

the Variability of Optical and Physical Properties of Aging Smoke Particles in Brazil," *Journal of Geophysical Research*, Vol. 104, No. D22, 1999, pp. 27473-27489. http://dx.doi.org/10.1029/1999JD900833

[12] T. F. Eck, B. N. Holben, D. E. Ward, M. M. Mukelabai, O. Dubovik, A. Smirnov, J. S. Schafer, N. C. Hsu, S. J. Piketh, A. Queface, J. Le Roux, R. J. Swap and I. Slutsker, "Variability of Biomass Burning Aerosol Optical Characteristics in Southern Africa during the SAFARI 2000 Dry Season Campaign and a Comparison of Single Scattering Albedo Estimates from Radiometric Measurements," *Journal of Geophysical Research*, Vol. 108 No. D13, 2003, p. 8477.

[13] T. F. Eck, B. N. Holben, J. S. Reid, O. Dubovic, A. Smirnov, N. T. O'Neill, I. Slutsker and S. Kinne, "Wavelength Dependence of the Optical Depth of Biomass Burning, Urban, and Desert Dust Aerosols," *Journal of Geophysical Research*, Vol. 104, No. D24, 1999, pp. 31333-31349. http://dx.doi.org/10.1029/1999JD900923

[14] A. Smirnov, A. Royer, N. T. O'Neill and A. Tarussov, "A Study of the Link between Synoptic Air Mass Type and Atmospheric Optical Parameters," *Journal of Geophysical Research*, Vol. 99, No. D10, 1994, pp. 20967-20982. http://dx.doi.org/10.1029/94JD01719

[15] N. C. Hsu, S. C. Tsay, M. D. King and J. R. Herman, "Deep-Blue retrievals of Asian aerosol properties during ACE-Asia," *IEEE Transactions on Geoscience and Remote Sensing*, Vol. 44, No. 11, 2006, pp. 3180-3195. http://dx.doi.org/10.1109/TGRS.2006.879540

[16] H. Moosmuller, R. K. Chakrabarty and W. P. Arnott, "Aerosol Light Absorption and Its Measurement: A Review," *Journal of Quantitative Spectroscopy and Radiative Transfer*, Vol. 110, NO. 11, 2009, pp. 844-878. http://dx.doi.org/10.1016/j.jqsrt.2009.02.035

[17] H. Moosmuller and R. K. Chakrabarty, "Technical Note: Simple Analytical Relationships between Angstrom Coefficients of Aerosol Extinction, Scattering, Absorption, and Single Scattering Albedo," *Atmospheric Chemistry and Physics*, Vol. 11, 2011, pp. 10677-10680. http://dx.doi.org/10.5194/acp-11-10677-2011

[18] K. Lewis, W. P. Arnott, H. Moosmuller and C. E. Wold, "Strong Spectral Variation of Biomass Smoke Light Absorption and Single Scattering Albedo Observed with a Novel Dual-Wavelength Photoacoustic Instrument," *Journal of Geophysical Research*, Vol. 113, No. D16, 2008. http://dx.doi.org/10.1029/2007JD009699

[19] O. Dubovik, B. N. Holben, Y. J. Kaufman, M. Yamasoe, A. Smirnov, D. Tanre and I. Slutsker, "Single-Scattering Albedo of Smoke Retrieved from the Sky Radiance and Solar Transmittance Measured from Ground," *Journal of Geophysical Research*, Vol. 103, No. D24, 1998, pp. 31901-31923. http://dx.doi.org/10.1029/98JD02276

[20] O. Dubovik and M. D. King, "A Flexible Inversion Algorithm for Retrieval of Aerosol Optical Properties from Sun and Sky Radiance Measurements," *Journal of Geophysical Research*, Vol. 105, No. D16, 2000, pp. 20673-20696. http://dx.doi.org/10.1029/2000JD900282

[21] M. I. Mishchenko, B. Cairns, G. Kopp, C. F. Schueler, B. A. Fafaul, J. E. Hansen, R. J. Hooker, T. Itchkawich, H. B. Maring and L. D. Travis, "Accurate Monitoring of Terrestrial Aerosols and Total Solar Irradiance—Introducing the Glory Mission," *Bulletin of the American Meteorological Society*, Vol. 88, No. 5, 2007, pp. 677-691. http://dx.doi.org/10.1175/BAMS-88-5-677

[22] L. Zhu, J. V. Martins and L. A. Remer, "Biomass Burning Aerosol Absorption Measurements with MODIS Using the Critical Reflectance Method," *Journal of Geophysical Research*, Vol. 116, No. D7, 2011. http://dx.doi.org/10.1029/2010JD015187

[23] A. Sanchez, T. F. Smith and W. F. Krajewski, "A Three-Dimensional Atmospheric Radiative Transfer Model Based on the Discrete-Ordinates Method," *Atmospheric Research*, Vol. 33, No. 1-4, 1994, pp. 283-308. http://dx.doi.org/10.1016/0169-8095(94)90024-8

[24] Z. Li, P. Goloub, C. Devaux, X. Gu, Y. Qiao, F. Zhao and H. Chen, "Aerosol Polarized Phase Function and Single-Scattering Albedo Retrieved from Ground-Based Measurements," *Atmospheric Research*, Vol. 71, No. 4, 2004, pp. 233-241. http://dx.doi.org/10.1016/j.atmosres.2004.06.001

[25] K. N. Liou and Y. Takano, "Light Scattering by Nonspherical Particles: Remote Sensing and Climatic Implications," *Atmospheric Research*, Vol. 31, No. 4, 1994, pp. 271-298. http://dx.doi.org/10.1016/0169-8095(94)90004-3

[26] A. Kylling, A.F. Bais, M. Blumthaler, J. Shreder and C. S. Zerefos, "UV Irradiances during the PAUR Campaign: Comparison between Measurement and Model Simulations," *Journal of Geophysical Research*, Vol. 103 No. D20, 1998, pp. 26051-26060.

[27] G. L. Schuster, O. Dubovik and B. N. Holben, "Angstrom Exponent and Bimodal Aerosol Size Distributions," *Journal of Geophysical Research*, Vol. 111, No. D7, 2006. http://dx.doi.org/10.1029/2005JD006328

[28] M. Hess, P. Koepke and I. Schult, "Optical Properties of Aerosols and Clouds: The Software Package OPAC," *Bulletin of the American Meteorological Society*, Vol. 79, No. 5, 1998, pp. 831-844.

[29] K. N. Liou, "An Introduction to Atmospheric Radiation," 2nd Edition, Academic Press, San Diego, 2002, p. 583.

[30] M. D. King and D. M. Byrne, "A Method for Inferring Total Ozone Content from Spectral Variation of Total Optical Depth Obtained with a Solar Radiometer," *Journal of the Atmospheric Sciences*, Vol. 33, No. 11, 1976, pp. 2242-2251. http://dx.doi.org/10.1175/1520-0469(1976)033<2242:AMFITO>2.0.CO;2

[31] T. F. Eck, B. N. Holben, O. Dubovic, A. Smirnov, I. Slutsker, J. M. Lobert and V. Ramanathan, "Column-Integrated Aerosol Optical Properties over the Maldives During the Northeast Mon-Soon for 1998-2000," *Journal of Geophysical Research*, Vol. 106, No. D22, 2001, pp. 28555-28566.

[32] T. F. Eck, B. N. Holben, D. E. Ward, O. Dubovic, J. S. Reid, A. Smirnov, M. M. Mukelabai, N. C. Hsu, N. T. O' Neil and I. Slutsker, "Characterization of the Optical Properties of Biomass Burning Aerosols in Zambia during the 1997 ZIBBEE Field Campaign," *Journal of Geophysical Research*, Vol. 106, No. D4, 2001, pp. 3425-

3448. http://dx.doi.org/10.1029/2000JD900555

[33] Y. J. Kaufman, "Aerosol Optical Thickness and Atmospheric Path Radiance," *Journal of Geophysical Research*, Vol. 98, No. D2, 1993, pp. 2677-2992. http://dx.doi.org/10.1029/92JD02427

[34] N. T. O'Neill, T. F. Eck, B. N. Holben, A. Smirnov, O. Dubovik and A. Royer, "Bimodal Size Distribution Influences on the Variation of Angstrom Derivatives in Spectral and Optical Depth Space," *Journal of Geophysical Research*, Vol. 106, No. D9, 2001, pp. 9787-9806. http://dx.doi.org/10.1029/2000JD900245

[35] N. T. O'Neill, T. F. Eck, A. Smirnov, B. N. Holben and S. Thulasiraman, "Spectral Discrimination of Coarse and Fine Mode Optical Depth," *Journal of Geophysical Research*, Vol. 198, No. D17, 2003, p. 4559.

[36] D. G. Kaskaoutis and H. D. Kambezidis, "Investigation into the Wavelength Dependence of the Aerosol Optical Depth in the Athens Area," *Journal of the Royal Meteorological Society*, Vol. 132, No. 620, 2006, pp. 2217-2234. http://dx.doi.org/10.1256/qj.05.183

[37] B. Schmid, D. A. Hegg, J. Wang, D. Bates, J. Redemann, P. B. Russell, J. M. Livingston, H. H. Jonsson, E. J. Welton, J. H. Seinfeld, R. C. Flagan, D. S. Covert, O. Dubovik, A. Jefferson, "Column Closure Studies of Lower Tropospheric Aerosol and Water Vapor During ACE-Asia Using Airborne Sun Photometer and Airborne *in Situ* and Ship-Based Lidar Measurements," *Journal of Geophysical Research*, Vol. 108 No. D23, 2003, p. 8656. http://dx.doi.org/10.1029/2002JD003361

[38] J. A. Martinez-Lozano, M. P. Utrillas, F. Tena, Pedros, R., J. Canada, J. V. Bosca and J. Lorente, "Aerosol Optical Characteristics from Summer Campaign in an Urban Coastal Mediterranean Area," *IEEE Transactions on Geoscience and Remote Sensing*, Vol. 39, No. 7, 2001, pp. 1573-1585. http://dx.doi.org/10.1109/36.934089

[39] D. G. Kaskaoutis, H. D. Kambezidis, N. Hatzianastassiou, P. G. Kosmopoulos and K. V. S. Badarinath, "Aerosol Climatology: Dependence of the Angstrom Exponent on Wavelength over Four AERONET Sites," *Atmospheric Chemistry and Physics*, Vol. 7, 2007, pp. 7347-7397. http://dx.doi.org/10.5194/acpd-7-7347-2007

[40] D. G. Kaskaoutis, H. D. Kambezidis, , N. Hatzianastassiou, P. G. Kosmopoulos and K. V. S. Badarinath, "Aerosol Climatology: On the Discrimination of Aerosol Types over Four AERONET Sites," *Atmospheric Chemistry and Physics Discussion*, Vol. 7, No. 3, 2007, pp. 6357-6411.

[41] J. W. Fitzgerald, "Approximation Formulas for the Equilibrium Size of an Aerosol Particle as a Function of Its Dry Size and Composition and Ambient Relative Humidity," *Journal of Applied Meteorology*, Vol. 14, No. 6, 1975, pp. 1044-1049. http://dx.doi.org/10.1175/1520-0450(1975)014<1044:AFFTES>2.0.CO;2

[42] I. N. Tang, "Chemical and Size Effects of Hygroscopic Aerosols on Light Scattering Coefficients," *Journal of Geophysical Research*, Vol. 101, No. D14, 1996, pp. 19245-19250. http://dx.doi.org/10.1029/96JD03003